# Multimodel Analysis of the Water Vapor Feedback in the Tropical Upper Troposphere

KEN MINSCHWANER

*Department of Physics, New Mexico Institute of Mining and Technology, Socorro, New Mexico*

ANDREW E. DESSLER

*Department of Atmospheric Sciences, Texas A&M University, College Station, Texas*

PARNCHAI SAWAENGPHOKHAI

*Department of Physics, New Mexico Institute of Mining and Technology, Socorro, New Mexico*

(Manuscript received 9 May 2005, in final form 10 January 2006)

ABSTRACT

Relationships between the mean humidity in the tropical upper troposphere and tropical sea surface temperatures in 17 coupled ocean–atmosphere global climate models were investigated. This analysis builds on a prior study of humidity and surface temperature measurements that suggested an overall positive climate feedback by water vapor in the tropical upper troposphere whereby the mean specific humidity increases with warmer sea surface temperature (SST). The model results for present-day simulations show a large range in mean humidity, mean air temperature, and mean SST, but they consistently show increases in upper-tropospheric specific humidity with warmer SST. The model average increase in water vapor at 250 mb with convective mean SST is 44 ppmv $K^{-1}$, with a standard deviation of 14 ppmv $K^{-1}$. Furthermore, the implied feedback in the models is not as strong as would be the case if relative humidity remained constant in the upper troposphere. The model mean decrease in relative humidity is $-2.3\% \pm 1.0\%$ $K^{-1}$ at 250 mb, whereas observations indicate decreases of $-4.8\% \pm 1.7\%$ $K^{-1}$ near 215 mb. These two values agree within the respective ranges of uncertainty, indicating that current global climate models are simulating the observed behavior of water vapor in the tropical upper troposphere with reasonable accuracy.

## 1. Introduction

Water vapor is generally recognized as the most important greenhouse gas in the earth's atmosphere (Held and Soden 2000), but the amount of water vapor in the atmosphere can be difficult to accurately predict. The temporal and spatial patterns of variability in water vapor are quite complex, involving orders of magnitude changes related to its sources, sinks, and long-range transport. One simplifying aspect is the exponential dependence of the saturation water vapor pressure on temperature through the Clausius–Clapeyron relation.

One of the earliest, approximate paradigms for gauging the response of water vapor in a changing climate was based on the assumption that relative humidity would be conserved, remaining fixed at the presently observed mean distribution (Manabe and Wetherald 1967). Thus, as the atmosphere initially warms because of increasing greenhouse gas abundances, both the saturation and specific humidities must rise proportionally, creating a strong positive feedback. The strength of this feedback is estimated to be about a factor of 2 in amplifying any $CO_2$-induced surface warming (Manabe and Wetherald 1967; Cubasch et al. 2001).

The physics of the water vapor budget of the lower troposphere involves a tight thermodynamic coupling of the surface and atmosphere, and a constant relative humidity assumption is plausible below about 700 mb (e.g., Betts and Ridgway 1988). In the middle and upper troposphere, the situation is more complicated; the magnitude of the water vapor feedback has been a matter of debate over the past 15 years (Lindzen 1990; Minschwaner and McElroy 1992; Sun and Lindzen 1993; Soden 1997; Yang and Tung 1998; Soden et al. 2002; Minschwaner and Dessler 2004). While the pri-

*Corresponding author address:* Dr. K. Minschwaner, Department of Physics, New Mexico Institute of Mining and Technology, Socorro, NM 87801.
E-mail: krm@kestrel.nmt.edu

mary source for water vapor above 700 mb is evaporation over the tropical oceans, the method of delivery involves the physics of atmospheric convection, such as the detrainment of vapor and evaporation of condensed water (Emanuel and Pierrehumbert 1996). The large-scale advection of water vapor away from convective source regions is also important in determining the distribution of humidity in the upper troposphere (Sherwood 1996; Dessler and Sherwood 2000).

Current climate models use a variety of schemes to simulate many of the complexities of these processes, with the outcome that the distribution of relative humidity remains approximately constant in the middle and upper troposphere (Soden et al. 2002). The degree to which upper-tropospheric relative humidity may vary with changing climate is an important issue because the radiative influence of water vapor is relatively large in the tropical upper troposphere (e.g., Pierrehumbert 1995). In this paper, we present an analysis of the water vapor feedback in the tropical upper troposphere as simulated by 17 coupled ocean–atmosphere climate models. The model simulations were performed in support of the Working Group One component of the Intergovernmental Panel on Climate Change (IPCC) Fourth Assessment Report. This multimodel output presents a unique opportunity for assessing the performance and sensitivity of the current generation of climate models.

## 2. Analysis method

The strength of the water vapor feedback in the IPCC models was inferred using methods described by Minschwaner and Dessler (2004). Folkins et al. (2002) showed that the mean budget of water vapor in the tropical upper troposphere (between about 10 and 14 km) can be approximated as a balance between the moisturizing influence of saturated detrainment from deep convection and the drying influence from large-scale subsidence. Their conclusions were drawn using a collection of satellite, aircraft, and balloonsonde measurements of tropical humidity. It should be emphasized that this balance does not capture spatial variability in upper-tropospheric humidity, nor can it adequately describe the water vapor distribution below 10 km, which is dependent on the evaporation of condensed cloud water. Rather, the Folkins model is an approximate description for the mean upper-tropospheric humidity (Folkins and Martin 2005), which is similar to the mean energy balance arising between radiative cooling and subsidence-induced warming (e.g., Betts and Ridgway 1988). Minschwaner and Dessler (2004) used a 1D radiative–convective model to show that the mean vertical distribution of water vapor in the tropical upper troposphere is consistent with both of these assumptions for energy and humidity balance. Within this framework, water vapor plays an active role through its influence on the mean rate of infrared cooling, which ultimately regulates the subsidence rate and the implied convective vertical mass fluxes and detrainment.

One of the more important variables that can be linked to tropical convection is the mean sea surface temperature (SST), and in particular, we are interested in the SST averaged over regions where convection is actually taking place. We used outgoing longwave radiation (OLR) to diagnose the spatial extent of convection and computed the monthly mean SST within tropical regions ($\pm 20°$ latitude) where the monthly mean OLR was less than 250 W $m^{-2}$. This OLR threshold corresponds to a maximum brightness temperature of about 258 K or an optically thick cloud with cloud-top pressure at 400 mb. Optically thinner clouds, or partial cloud cover, would correspond to a higher altitude for the same OLR.

Shown in Fig. 1 is a contour plot of the July SST for one of the models. Also outlined is the 250 W $m^{-2}$ OLR contour where it occurs within $\pm 20°$ latitude. Regions within these contours are where SSTs are averaged in our analysis to define the convective mean sea surface temperature, $\overline{\mathrm{SST}}_c$. It can be seen in Fig. 1 that the OLR threshold generally encloses the warmest SST and that this is consistent with the tendency for deep convection to occur over the warmest ocean surface (Ramage 1968). The correlation is not perfect, however, which is not surprising given that there are other factors (such as SST gradients) that can influence spatial patterns of tropical convection (e.g., Lindzen and Nigam 1987). What is important to bear in mind for the purposes of this study is that $\overline{\mathrm{SST}}_c$ represents one measure of the forcing influences on tropical convection and that we assume $\overline{\mathrm{SST}}_c$ will be positively correlated with global mean temperatures under a climate change scenario.

The model outputs used here were taken from IPCC simulations and are the twentieth-century, all-forcings runs (20C3M). SST, model OLR, and monthly mean values of specific humidity and air temperature at the 250-mb model level were used from a 20-yr period between 1980 and 2000. As recommended by the IPCC Working Group One (see online at http://www-pcmdi.llnl.gov/ipcc/info_for_analysts.php), this simulation and time period were adopted to best represent the mean climate state for comparisons against contemporary observations. We obtained the model output from the archives of the Program for Climate Model Diagnostic

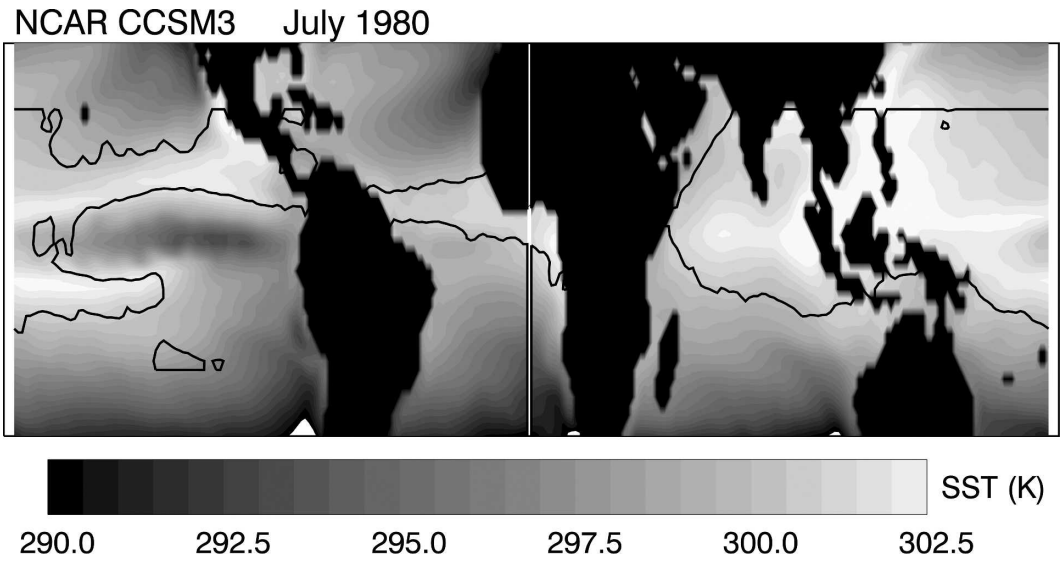


FIG. 1. The shaded contour plot of mean SST for the July 1980 simulation of the 20C3M from the Community Climate System Model version 3 (CCSM3). The black contour line shows the area enclosed by OLR $<250$ W m$^{-2}$ within the tropical latitudes of $\pm 20°$.

and Intercomparison (PCMDI) at the Lawrence Livermore National Laboratory. Table 1 lists the model names and references corresponding to the model numbers presented in our analysis. The ordering of the models is random and should not be taken as any indication of performance since we are exclusively interested in the ensemble means and variances among models.

Figures 2 and 3 show how the analysis is carried out for one model. Monthly mean specific humidity, relative humidity, and $\overline{\mathrm{SST}}_c$ are computed as a first step. For specific and relative humidities, the spatial averaging includes all model grid points between 20°S and 20°N on the model pressure level at 250 mb. Relative humidities are computed using specific humidities and air temperature at 250 mb. Saturation vapor pressures are computed over ice (Murray 1967). It should be noted that relative humidity computed using monthly mean specific humidity and monthly mean air temperature can differ from the true mean relative humidity according to the variance in specific humidity and air temperature (and corresponding saturation humidity). For symmetric temperature and specific humidity distribution functions, the true mean relative humidity generally tends to be larger than the value calculated based on mean variables. We estimated this effect assuming Gaussian temperature and specific humidity distributions with means and half widths of $232 \pm 2$ K and $260 \pm 40$ ppmv, respectively. These values represent typical model means and variances in the upper troposphere (Fig. 2). The average difference between the two methods of calculating relative humidity was 2.3%.

Figure 2 presents the time series for model 1 as a typical example. Also shown are the annual mean cycles calculated from each time series, so that interannual anomalies can be seen as departures from the annual mean cycle. Clearly, interannual anomalies in specific humidity are positively correlated with $\overline{\mathrm{SST}}_c$

TABLE 1. Models used in the analysis.

| Number | Model name | Reference |
|---|---|---|
| 1 | CCSM3 | Collins et al. (2006) |
| 2 | UKMO-HadCM3 | Gordon et al. (2000) |
| 3 | ECHAM5/MPI-OM | Jungclaus et al. (2006) |
| 4 | GISS-AOM | Russell et al. (1995) |
| 5 | CSIRO-Mk3.0 | Gordon et al. (2002) |
| 6 | GFDL-CM2.0 | Delworth et al. (2006) |
| 7 | CNRM-CM3 | Salas-Mélia et al. (2005, manuscript submitted to *Climate Dyn.*) |
| 8 | MIROC3.2(medres) | K-1 Model Developers (2004) |
| 9 | FGOALS-g1.0 | Yu et al. (2004) |
| 10 | INM-CM3.0 | Diansky and Volodin (2002) |
| 11 | GFDL-CM2.1 | Delworth et al. (2006) |
| 12 | IPSL-CM4 | Marti et al. (2005) |
| 13 | GISS-ER | Schmidt et al. (2006) |
| 14 | MIROC3.2(hires) | K-1 Model Developers (2004) |
| 15 | GISS-EH | Schmidt et al. (2006) |
| 16 | PCM | Washington et al. (2000) |
| 17 | MRI-CGCM2.3.2 | Yukimoto et al. (2001) |

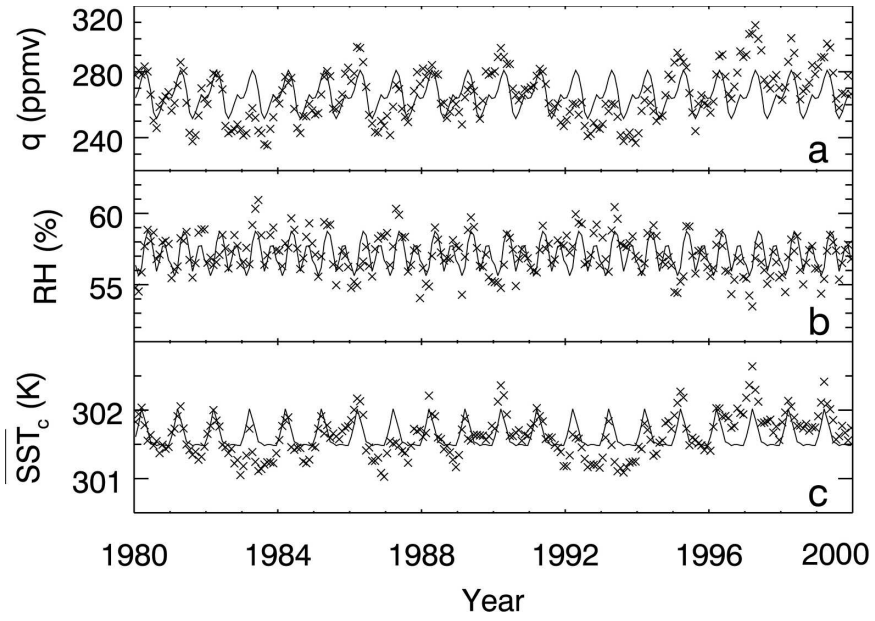


FIG. 2. (a) Time series of monthly mean tropical specific humidity at 250 mb from model 1 for the 20C3M simulation (xs). The solid curve shows the repeating annual cycle computed from the monthly means. (b) Same as in (a), but for RH at 250 mb. (c) Same as in (a), but for SSTs; the mean is computed only over regions where the monthly mean OLR is less than 250 W $m^{-2}$.

anomalies, and anomalies in relative humidity appear to be anticorrelated with $\overline{SST}_c$.

The above correlations are presented in Fig. 3, which shows scatterplots of the interannual anomalies from Fig. 2. For consistency with previous analyses, we allow for a 1-month phase lag between humidity variations and $\overline{SST}_c$ in order to account for the response time scales between SST, boundary layer moist entropy, convection, and upper-tropospheric humidity (Minschwaner and Dessler 2004). For both specific and relative humidity anomalies in Fig. 3, the correlations with SST are well represented by linear least squares fits with slopes of 47.0 ± 3.4 ppmv $K^{-1}$ and −2.9 ± 0.38% $K^{-1}$, respectively. Quoted uncertainties in this case and in all subsequent analyses refer to the $1\sigma$ uncertainty in the fitted slope (Taylor 1982).

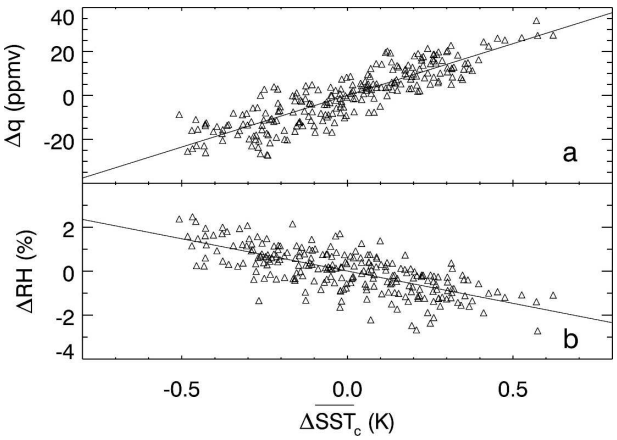


FIG. 3. (a) A scatterplot of monthly mean anomalies in tropical specific humidity at 250 mb versus anomalies in convective mean SST (triangles) for model 1 over the 1980–2000 period of the 20C3M simulation. The solid line shows the least squares linear fit. (b) Same as in (a), but for RH.

Figure 3a shows that this particular model should display a positive water vapor feedback, and Fig. 3b suggests that the implied feedback is not as large as the case of constant relative humidity. However, there are underlying assumptions in our method that might bias the implied feedback. We explore the sensitivity of our results to these assumptions in the collective analysis of the models that follows.

## 3. Results for all models

The above method was applied to output from all other models, and the slopes of the linear regressions between humidity and $\overline{SST}_c$ anomalies are summarized in Fig. 4. While all of the models display a positive correlation between specific humidity and convective mean SST, the range of slopes is quite large and varies

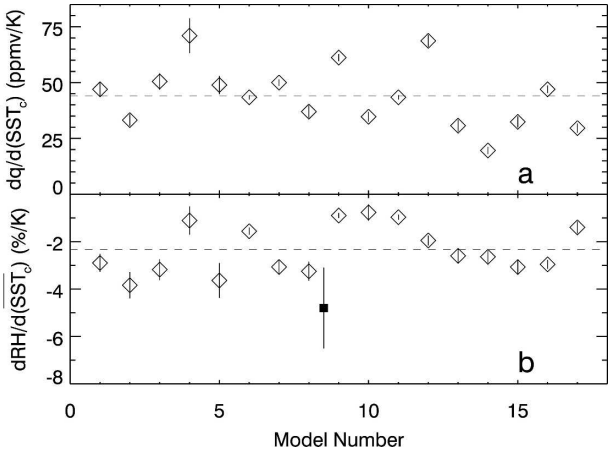


FIG. 4. A summary of model correlations for (a) specific humidity and (b) RH at 250 mb. Each model result is indicated by diamonds, with $1\sigma$ uncertainties indicated. Both plots show model ensemble means as dashed lines. In (b), the measured result at 215 mb is indicated by the filled square with $1\sigma$ uncertainty.

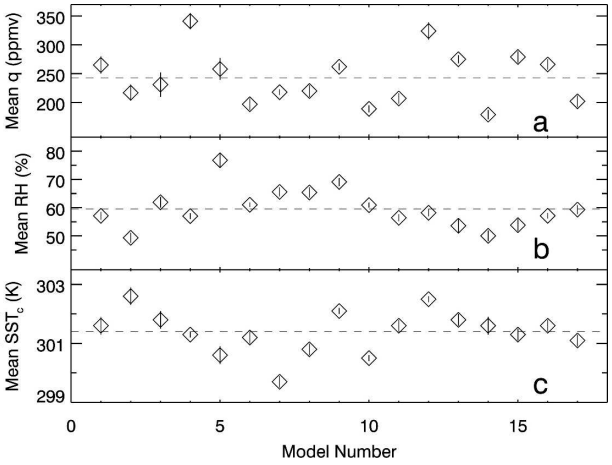


FIG. 5. A summary of model means for 250-mb (a) specific humidity and (b) RH, and (c) convective mean SST, all indicated by diamonds with $1\sigma$ standard deviations. All plots show model ensemble means as dashed lines.

from 20 to 70 ppmv $K^{-1}$. The mean slope for all of the models is 44 $\pm$ 14 ppmv $K^{-1}$ ($1\sigma$ standard deviation in the ensemble mean).

For relative humidity, all the of models show a small negative correlation with convective mean SST (Fig. 4b). The range of slopes is also large, however, from $-1\%$ to $-4\%$ $K^{-1}$. The mean for all models is $-2.3 \pm 1.0\%$ $K^{-1}$, which agrees marginally with an observed value of $-4.8 \pm 1.7\%$ $K^{-1}$ at 215 mb ($1\sigma$ uncertainty in the observed value). This measured correlation was obtained using relative humidity data from the Microwave Limb Sounder, and OLR and SST from the National Centers for Environmental Prediction–National Center for Atmospheric Research (NCEP–NCAR) reanalysis (Kalnay et al. 1996) over the period from 1992 to 1997 (Minschwaner and Dessler 2004).

The consistency between all models for the changes in specific and relative humidity is surprising in light of the large differences in convective parameterizations, transport, spatial resolution, and mean states. The variation between mean model states can be seen by comparing the 20-yr mean specific humidity, relative humidity, and $\overline{\text{SST}}_c$ for all models, as shown in Fig. 5. The range in specific humidities at 250 mb is found to be nearly a factor of 2 (Fig. 5a). We examined the magnitude of mean specific humidities, as well as humidity–SST correlations, for any correspondence with model spatial or vertical resolution and found none.

Relative humidities show a smaller variation ($\pm 25\%$), and there is no simple 1:1 correspondence between higher-than-average specific humidity and higher relative humidity. It appears that most of the variation between model specific humidities at 250 mb is related to variations in temperature at 250 mb (not shown).

In regard to the convective mean model SSTs, we also found a large variation between model 20-yr means (Fig. 5c). The range in $\overline{\text{SST}}_c$ is about 3 K, but the ensemble mean of 301.4 K is in good agreement with the mean observed value used in the analysis by Minschwaner and Dessler (2004) for the period 1992–97. The models generally have similar mean boundary layer relative humidities and the thermal structures are close to moist pseudoadiabatic; therefore, the $\overline{\text{SST}}_c$ variations in Fig. 5c can provide a very rough indication of each model's departure from the ensemble mean in upper-tropospheric air temperature. For example, in model 2, we find a specific humidity that is slightly below the ensemble mean. In contrast, this model's $\overline{\text{SST}}_c$ is significantly above the mean, leading to a warmer upper-tropospheric air temperature and higher saturation humidity. The combined effect produces the smallest mean relative humidity among all of the models (49%). Note, however, that this is only an approximate relationship since all of the models do not follow exactly the same mean tropospheric lapse rate.

Sensitivities for the slopes of the linear correlations shown in Fig. 4 were tested by varying the latitudinal averaging boundaries, OLR threshold for SST, time series period, and phase lag between SST and humidity variations. Table 2 presents the largest response magnitude for the indicated change, expressed as a percentage of the result obtained from our standard analysis parameters. For example, the first entry shows that the use of a different 20-yr time period (1960–80) produces

TABLE 2. The maximum change in implied $H_2O$ feedback due to changes in assumed analysis parameters.

| Change | $dq/d(\overline{\text{SST}}_c)$ | $d\text{RH}/d(\overline{\text{SST}}_c)$ |
|---|---|---|
| Time period (1960–80) | 9% | 23% |
| Latitude (±30°) | 68%* | 84%* |
| OLR (240, 260 W $m^{-2}$) | 4% | 12% |
| Zero phase lag | 4% | 11% |
| Average over all tropical SST | 49% | 26% |
| Include annual cycle | 60%* | 64%* |

* Significant decrease in correlation coefficient.

maximum changes of 9% and 23% in the regression coefficients.

We found the largest changes when latitude boundaries were increased from ±20° to ±30° latitude. For this case, all of the fitted slopes became smaller and the linear correlation coefficients decreased. We believe this to be a result of including model grid points that were more often under the influence of an extratropical climate regime, where the above assumptions for energy and moisture balance may not be entirely appropriate. In cases where the OLR thresholds for SST averaging were altered (from 240 to 260 W $m^{-2}$) or the phase lag was removed between humidity and SST, we found no systematic changes in the humidity–SST regression and the effects were generally small.

For the case where the OLR threshold for SST averaging was removed completely (averaging over all tropical SSTs), we found maximum changes of 49% and 26% in the regression coefficients for specific and relative humidities, respectively. Both slope magnitudes were systematically larger in this case; that is, $dq/d(\overline{\text{SST}})$ was more positive and $d\text{RH}/d(\overline{\text{SST}})$ was more negative for most models. The effect arises from differences between the magnitudes of anomalies in convective mean SSTs as opposed to tropical mean SSTs. In general, when convective mean SSTs warm up or cool down, the overall tropical mean SST behaves similarly but with a smaller amplitude. Thus, the range of the independent variable in the linear regression is reduced while the dependent variable is unchanged, which produces larger slope magnitudes. Clearly, the magnitude (but not the sign) of the implied water vapor feedback in the models can vary according to the SST index used. The convective mean SST is used here primarily because of evidence that convection plays a dominant role in regulating the mean humidity of the upper troposphere.

The final entry in Table 2 shows the effect of retaining annual cycles in humidity and convective mean SST. Annual cycles are removed in our standard analysis in order to focus on interannual anomalies. This choice was guided by prior studies showing that annual variability may not be a suitable surrogate for climate change (e.g., Bony et al. 1995) even when variables are averaged over an entire climate domain such as the Tropics (Lindzen et al. 1995). Table 2 shows that including annual cycles in humidity and SST produced changes of up to 64% in the fitted slope, but more importantly, we found a smaller linear correlation coefficient in this case for all models. The changes in slope were not systematic; some models displayed a larger slope while others produced a smaller slope with the annual cycle included.

On the other hand, the interannual tropical variability used here is dominated by the effects of El Niño–Southern Oscillation (ENSO), and the suitability of ENSO as a surrogate for greenhouse-induced climate change has been questioned. Del Genio (2002) showed that modeled changes in the global distribution of upper-tropospheric humidity differed significantly between ENSO and doubled $CO_2$ simulations. Lau et al. (1996) found that the local water vapor feedbacks and cloud radiative forcings during ENSO were largely determined by basinwide dynamical responses to SST forcing. However, Lau et al. did note that the use of domain averages (e.g., global or tropical rather than correlations at individual grid points) during ENSO provides at least the possibility for meaningful climate change estimates.

We compared the interannual humidity–SST correlation with that obtained under a changing climate scenario for four of the models that cover a range of specific and relative humidity responses (models 2, 10, 12, and 13). The climate change scenario was based on greenhouse gas emissions from Special Report on Emission Scenarios (SRES A2; Nakicenovic et al. 2000), where the models were initialized using the end of the 20C3M run representing present-day conditions. Figure 6 shows annual and tropical mean vertical profiles of relative humidity for years 2010 and 2100. We find that all four models maintain a constant relative humidity below about 600 mb to within a few tenths of a percent. Between 500 and 200 mb, model relative humidities are smaller in year 2100 compared to 2010 (though specific humidity still increases, i.e., the water vapor feedback is positive). Above about 150 mb, relative humidities are larger in year 2100 compared to 2010. Note that these changes cannot generally be described by a single upward displacement of the relative humidity profile. In two of the models, the maximum in relative humidity remains near 150 mb but decreases significantly in magnitude.

The above analysis can be extended for comparison with the water vapor feedback inferred from interan-

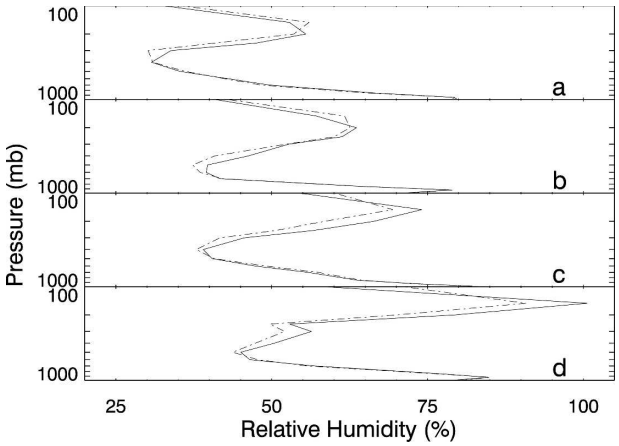


FIG. 6. Vertical profiles of tropical mean RH for models (a) 2, (b) 10, (c) 12, and (d) 13 in the annual mean for year 2010 (solid line) and 2100 (dashed–dotted line).

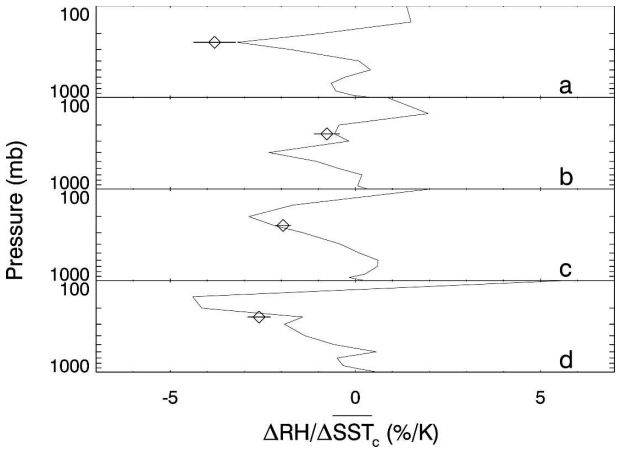


FIG. 7. Differences in the relative humidities shown in Fig. 6, divided by corresponding changes in convective mean SST over the same time period (2010–2100). Also shown are the inferred values at 250 mb (diamonds) obtained using a linear fit to interannual variations in RH and $\overline{\mathrm{SST}}_c$ between 1980 and 2000.

nual variations in relative humidity and $\overline{\mathrm{SST}}_c$. The increase in $\overline{\mathrm{SST}}_c$ between years 2010 and 2100 ranged from 2.1 to 2.7 K in the models. If we divide the relative humidity changes between years 2010 and 2100 by the corresponding changes in $\overline{\mathrm{SST}}_c$, we obtain vertical profiles of $\Delta\mathrm{RH}/\Delta\overline{\mathrm{SST}}_c$, shown in Fig. 7. Also plotted are the values obtained at 250 mb using the linear regression of interannual variations. Humidity changes inferred from interannual variability are larger than the climate change simulation for three of the models but smaller for one of the models. Judging from these four cases where the level of agreement is at or near the uncertainties, we conclude that using interannual anomalies in humidity may be a reasonable proxy for gauging the tropical mean water vapor feedback at 250 mb.

## 4. Discussion

The physics behind the tendency for positive water vapor feedbacks that are weaker than given by fixed relative humidity was explored by Minschwaner and Dessler (2004) using a 1D radiative–convective framework. It was found that convection penetrates to higher altitudes as the surface warms, and the convective mass flux is larger in the upper troposphere (Mitchell and Ingram 1992) even though the vertically integrated convective flux actually weakens (Minschwaner and Dessler 2004). The enhanced drying through subsidence is more than counteracted, however, by an increased delivery of water vapor through saturated detrainment at warmer temperatures in the upper troposphere. Thus, some aspects of previously proposed convective drying mechanisms may be operating in the models to cause decreases in relative humidity, but they are not strong enough to overcome the Clausius–Clapeyron equation and force the feedback to be negative [i.e., $dq/d(\overline{\mathrm{SST}}_c)$ is positive for all models]. These results might appear to conflict with the conclusion by Soden et al. (2002) that the cooling and drying response of the upper troposphere following the eruption of Mount Pinatubo was consistent with a constant relative humidity. However, the Television Infrared Observation Satellite (TIROS) Operational Vertical Sounder (TOVS) 6.7-$\mu$m radiances used by Soden et al. are sensitive to relative humidity averaged over a broad layer from 200 to 500 mb, rather than a specific level at 250 mb used here. If the TOVS weighting function (Soden and Fu 1995) is applied to the relative humidity changes indicated in Fig. 7, we would find changes that are significantly smaller than those found at 250 mb and are very close to zero.

In Fig. 8, we show the results for fractional changes in specific and relative humidities, both as functions of changes in $\overline{\mathrm{SST}}_c$. Also plotted in Fig. 8 is a result from observations at 215 mb (Minschwaner and Dessler 2004), where the specific humidities are from the Halogen Occultation Experiment (HALOE). The latter data are not included in Fig. 5a because large vertical gradients in specific humidity make comparisons between absolute values at 215 and 250 mb suspect; a comparison of fractional changes is less impacted by this pressure difference. In addition, there is a known dry bias in HALOE water vapor below the tropopause (Kley et al. 2000). We find that the observations tend to imply a smaller fractional increase in specific humidity and a corresponding larger fractional decrease in relative humidity than are simulated by many of the models.

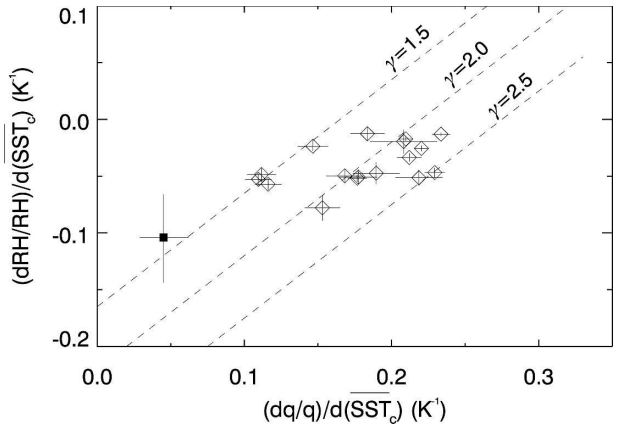


FIG. 8. Model sensitivities at 250 mb for fractional changes in specific humidity with convective mean SST, plotted against fractional changes in relative humidity with convective mean SST (diamonds). The solid square is a value obtained from observed variations at 215 mb. The dashed lines indicate the relationship expected between the abscissa and ordinate for indicated values of $\gamma = dT_{250}/d(\overline{\mathrm{SST}}_c)$ (see text).

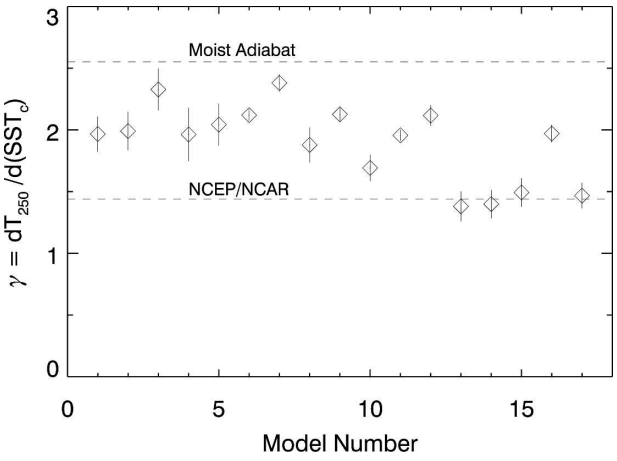


FIG. 9. Model values for $\gamma = dT_{250}/d(\overline{\mathrm{SST}}_c)$ obtained from interannual variations over the period 1980–2000 (diamonds with $1\sigma$ uncertainties). The upper and lower dashed lines represent the moist adiabatic value and the result from the NCEP–NCAR reanalysis, respectively.

Relative and specific humidities should be anticorrelated for fixed air temperature; thus, one might expect to find that models with the largest fractional increase in specific humidity would also show the smallest fractional decrease in relative humidity. In fact, the correlation should hold only for the case where temperatures at 250 mb are positively correlated with SST through the lapse rate. This can be seen by writing

$$\frac{d\ln(\mathrm{RH}_{250})}{d(\overline{\mathrm{SST}}_c)} = \frac{d\ln(q_{250})}{d(\overline{\mathrm{SST}}_c)} - \frac{d\ln[q^*(T_{250})]}{d(\overline{\mathrm{SST}}_c)}, \qquad (1)$$

where $\mathrm{RH}_{250}$, $q_{250}$, and $q^*(T_{250})$ are the relative humidity, specific humidity, and saturation humidity at 250 mb, respectively. The last term may be expanded as

$$\frac{d\ln[q^*(T_{250})]}{d(\overline{\mathrm{SST}}_c)} = \frac{d\ln[q^*(T_{250})]}{dT_{250}} \frac{dT_{250}}{d(\overline{\mathrm{SST}}_c)}. \qquad (2)$$

The first factor on the right-hand side is approximately constant according to the Clausius–Clapeyron relation, and the second factor is the sensitivity of upper-tropospheric temperature to convective mean SST, which ultimately is related to changes in the mean lapse rate. We define $\gamma = dT_{250}/d(\overline{\mathrm{SST}}_c)$, then

$$\frac{d\ln(\mathrm{RH}_{250})}{d(\overline{\mathrm{SST}}_c)} = \frac{d\ln(q_{250})}{d(\overline{\mathrm{SST}}_c)} - \frac{b}{T_{250}^2}\gamma \qquad (3)$$

with $b = 6142$ K (Johnson et al. 2001).

For a fixed value of $\gamma$ and small fractional changes in $T_{250}$, we should find that Eq. (3) describes a line in Fig. 8 with a slope of unity and an intercept determined primarily by $\gamma$. Plotted in Fig. 8 are lines corresponding to $\gamma = 1.5$, 2, and 2.5. Most of the models are consistent with a $\gamma$ of approximately 2, which is slightly below the moist pseudoadiabatic value of about 2.5. We find that most of the differences between models in relation to their specific versus relative humidity responses can be traced to differences in model values of $\gamma$.

The variation in $\gamma$ between models is more easily seen in Fig. 9, which also includes the moist adiabatic limit and a value of 1.5 obtained using the NCEP–NCAR reanalysis data from 1990 to 1999 (Kalnay et al. 1996). The models generally fall within these two extremes, tending to be less sensitive than the moist pseudoadiabat but more sensitive than the NCEP–NCAR reanalysis data. A comparison of Figs. 4 and 9 shows very little correspondence between the implied water vapor feedback $[dq/d(\overline{\mathrm{SST}}_c)]$ and the temperature sensitivity ($\gamma$). One likely explanation is that the coupling between the budgets for water vapor and thermodynamic balance in the upper troposphere varies according to the particular convective parameterization used in any given model; thus, $dq_{250}/d(\overline{\mathrm{SST}}_c)$ and $dT_{250}/d(\overline{\mathrm{SST}}_c)$ appear to vary independently among the models, and the results for $d\mathrm{RH}/d(\overline{\mathrm{SST}}_c)$ in Fig. 4 reflect the net outcome of these two effects according to Eq. (3). It should also be noted that the temperature sensitivity is a function of our choice for SST averaging. If, for example, SST is averaged over the entire $\pm 20°$ domain without regard to OLR, then both the NCEP–NCAR data and most of the models show a value of $dT_{250}/d\mathrm{SST}$ of $\simeq 2.2$. This larger temperature sensitivity arises from the smaller magnitude of SST variations in the tropical mean compared to more restricted regions of active convection and is consistent with the larger hu-

midity sensitivities noted previously in connection with overall mean tropical SSTs.

## 5. Conclusions

The water vapor feedback in the tropical upper troposphere was investigated using present-day simulations from 17 coupled ocean–atmosphere global climate models. All models show tendencies for a positive feedback at 250 mb, with specific humidities increasing as the mean sea surface temperature in convective regions becomes warmer. The ensemble mean correlation for specific humidity is 44 ppmv $K^{-1}$. Furthermore, all of the models show a decrease in relative humidity with increasing SST, with an ensemble mean correlation of $-2.3\%$ $K^{-1}$. Although the magnitude of the relative humidity decrease is smaller than inferred by measurements ($-4.8\%$ $K^{-1}$), it is within the limit of combined uncertainties. Changes in upper-tropospheric specific humidity in the models were not systematically related to tropical mean lapse rate changes, but changes in relative humidity could be attributed to the net effect of specific humidity and mean lapse rate changes. Finally, the feedbacks inferred using interannual anomalies in humidity and convective mean SST were consistent with values obtained in climate change simulations.

*Acknowledgments.* This work was supported by NASA Office of Earth Science Grant NNG04GM75G to New Mexico Tech and the University of Maryland. A. E. Dessler also acknowledges support from a NASA ACMAP Grant to the University of Maryland and Texas A&M University. We thank Steve Sherwood, Anthony Del Genio, and an anonymous reviewer for their thoughtful evaluations and suggestions that improved this paper. We acknowledge the international modeling groups for providing their data for analysis, the Program for Climate Model Diagnosis and Intercomparison (PCMDI) for collecting and archiving the model data, the JSC/CLIVAR Working Group on Coupled Modeling (WGCM) and their Coupled Model Intercomparison Project (CMIP) and Climate Simulation Panel for organizing the model data analysis activity, and the IPCC WG1 TSU for technical support. The IPCC Data Archive at Lawrence Livermore National Laboratory is supported by the Office of Science, U.S. Department of Energy.

## REFERENCES

Betts, A. K., and W. Ridgway, 1988: Coupling of the radiative, convective, and surface fluxes over the equatorial Pacific. *J. Atmos. Sci.,* **45,** 522–536.

Bony, S., J. P. Duvel, and H. Letreut, 1995: Observed dependence of the water vapor and clear-sky greenhouse effect on sea surface temperature: Comparison with climate warming experiments. *Climate Dyn.,* **11,** 307–320.

Collins, W. D., and Coauthors, 2006: The Community Climate System Model version 3 (CCSM3). *J. Climate,* **19,** 2122–2143.

Cubasch, U., and Coauthors, 2001: Projections of future climate change. *Climate Change 2001: The Scientific Basis,* J. T. Houghton et al., Eds., Cambridge University Press, 525–582.

Del Genio, A. D., 2002: The dust settles on water vapor feedback. *Science,* **296,** 665–666.

Delworth, T. L., and Coauthors, 2006: GFDL's CM2 global coupled climate models. Part I: Formulation and simulation characteristics. *J. Climate,* **19,** 643–674.

Dessler, A. E., and S. C. Sherwood, 2000: Simulations of tropical upper tropospheric humidity. *J. Geophys. Res.,* **105,** 20 155–20 163.

Diansky, N. A., and E. M. Volodin, 2002: Simulation of present-day climate with a coupled atmosphere–ocean general circulation model. *Izv. Atmos. Oceanic Phys.,* **38,** 732–747.

Emanuel, K. A., and R. T. Pierrehumbert, 1996: Microphysical and dynamical control of tropospheric water vapor. *Clouds, Chemistry, and Climate,* P. J. Crutzen and V. Ramanathan, Eds., NATO ASI Series, Vol. 135, Springer-Verlag, 17–28.

Folkins, I., and R. V. Martin, 2005: The vertical structure of tropical convection and its impact on the budgets of water vapor and ozone. *J. Atmos. Sci.,* **62,** 1560–1573.

——, K. K. Kelly, and E. M. Weinstock, 2002: A simple explanation for the increase in relative humidity between 11 and 14 km in the Tropics. *J. Geophys. Res.,* **107,** 4736, doi:10.1029/2002JD002185.

Gordon, C., C. Cooper, C. A. Senior, H. Banks, J. M. Gregory, T. C. Johns, J. F. B. Mitchell, and R. A. Wood, 2000: The simulation of SST, sea ice extents and ocean heat transports in a version of the Hadley Centre coupled model without flux adjustments. *Climate Dyn.,* **16,** 147–168.

Gordon, H. B., and Coauthors, 2002: The CSIRO Mk3 climate system model. CSIRO Atmospheric Research Tech. Doc. 60, 130 pp.

Held, I. M., and B. J. Soden, 2000: Water vapor feedback and global warming. *Annu. Rev. Energy Environ.,* **25,** 441–475.

Johnson, D. G., K. W. Jucks, W. A. Traub, and K. V. Chance, 2001: Isotopic composition of stratospheric water vapor: Implications for transport. *J. Geophys. Res.,* **106,** 12 219–12 226.

Jungclaus, J. H., and Coauthors, 2006: Ocean circulation and tropical variability in the coupled model ECHAM5/MPI-OM. *J. Climate,* **19,** 3952–3972.

K-1 Model Developers, 2004: K-1 coupled model (MIROC) description. K-1 Tech. Rep., Center for Climate System Research, University of Tokyo, 34 pp.

Kalnay, E., and Coauthors, 1996: The NCEP/NCAR 40-Year Reanalysis Project. *Bull. Amer. Meteor. Soc.,* **77,** 437–471.

Kley, D., J. M. Russell III, and C. Phillips, Eds., 2000: SPARC assessment of upper tropospheric and stratospheric water vapour. SPARC Rep. 2, World Climate Research Program 113, WMO Tech. Doc. 1043, 312 pp.

Lau, K. M., C. H. Ho, and M. D. Chou, 1996: Water vapor and cloud feedback over the tropical oceans: Can we use ENSO as a surrogate for climate change? *Geophys. Res. Lett.,* **23,** 2971–2974.

Lindzen, R. S., 1990: Some coolness concerning global warming. *Bull. Amer. Meteor. Soc.,* **71,** 288–299.

——, and S. Nigam, 1987: On the role of sea surface temperature

gradients in forcing low-level winds and convergence in the tropics. *J. Atmos. Sci.,* **44,** 2418–2436.

——, B. Kirtman, D. Kirk-Davidoff, and E. K. Schneider, 1995: Seasonal surrogate for climate. *J. Climate,* **8,** 1681–1684.

Manabe, S., and R. T. Wetherald, 1967: Thermal equilibrium of the atmosphere with a given distribution of relative humidity. *J. Atmos. Sci.,* **24,** 241–259.

Marti, O., and Coauthors, 2005: The new IPSL climate system model: IPSL-CM4. IPSL Tech. Rep., Institut Pierre Simon Laplace des Sciences de l'Environnement Global, Paris, France, 86 pp.

Minschwaner, K., and M. B. McElroy, 1992: Radiative constraints on the energy budget of the tropical atmosphere. *Planet. Space Sci.,* **40,** 1585–1597.

——, and A. E. Dessler, 2004: Water vapor feedback in the tropical upper troposphere: Model results and observations. *J. Climate,* **17,** 1272–1282.

Mitchell, J. F. B., and W. J. Ingram, 1992: Carbon dioxide and climate: Mechanisms of changes in cloud. *J. Climate,* **5,** 5–21.

Murray, F. W., 1967: On the computation of saturation vapor pressure. *J. Appl. Meteor.,* **6,** 203–204.

Nakicenovic, N., and Coauthors, Eds., 2000: *Special Report on Emissions Scenarios.* Cambridge University Press, 599 pp.

Pierrehumbert, R. T., 1995: Thermostats, radiator fins, and the local runaway greenhouse. *J. Atmos. Sci.,* **52,** 1784–1806.

Ramage, C. S., 1968: Role of a tropical "maritime continent" in the atmospheric circulation. *Mon. Wea. Rev.,* **96,** 365–370.

Russell, G. L., J. R. Miller, and D. Rind, 1995: A coupled atmosphere–ocean model for transient climate change studies. *Atmos.–Ocean,* **33,** 683–730.

Schmidt, G. A., and Coauthors, 2006: Present-day atmospheric simulations using GISS ModelE: Comparison to in situ, satellite, and reanalysis data. *J. Climate,* **19,** 153–192.

Sherwood, S. C., 1996: Maintenance of the free-tropospheric tropical water vapor distribution. Part I: Clear regime budget. *J. Climate,* **9,** 2903–2918.

Soden, B. J., 1997: Variations in the tropical greenhouse effect during El Niño. *J. Climate,* **10,** 1050–1055.

——, and R. Fu, 1995: A satellite analysis of deep convection, upper tropospheric humidity, and the greenhouse effect. *J. Climate,* **8,** 2333–2351.

——, R. T. Wetherald, G. L. Stenchikov, and A. Robock, 2002: Global cooling after the eruption of Mount Pinatubo: A test of climate feedback by water vapor. *Science,* **296,** 727–730.

Sun, D., and R. S. Lindzen, 1993: Water vapor feedback and the ice-age snowline record. *Ann. Geophys.,* **11,** 204–215.

Taylor, J. R., 1982: *An Introduction to Error Analysis: The Study of Uncertainties in Physical Measurements.* University Science Books, 270 pp.

Washington, W. M., and Coauthors, 2000: Parallel climate model (PCM) control and transient simulations. *Climate Dyn.,* **16,** 755–774.

Yang, H., and K. K. Tung, 1998: Water vapor, surface temperature, and the greenhouse effect—A statistical analysis of tropical mean data. *J. Climate,* **11,** 2686–2697.

Yu, Y., X. Zhang, and Y. Guo, 2004: Global coupled ocean–atmosphere general circulation models in LASG/IAP. *Adv. Atmos. Sci.,* **21,** 444–455.

Yukimoto, S., N. Akira, T. Uchiyama, and S. Kusunoki, 2001: Climate change of the twentieth through twenty-first centuries simulated by the MRI-CGCM2.3. *Pap. Meteor. Geophys.,* **51,** 47–88.